# A Computational Study of Ethylene C–H Bond Activation by [Cp*Ir(PR3)]

Kevin Smith, Rinaldo Poli, Jeremy Harvey

# A Computational Study of Ethylene C–H Bond Activation by [Cp*Ir($PR_3$)]

Kevin M. Smith,[a,b] Rinaldo Poli,*[a] and Jeremy N. Harvey*[c]

[a] K. M. Smith, R. Poli
Laboratoire de Synthèse et d'Electrosynthèse Organométallique,
Faculté des Sciences "Gabriel", Université de Bourgogne,
6 Boulevard Gabriel, 21100, Dijon, France
e-mail: Rinaldo-Poli@u-bourgogne.fr

[b] K. M. Smith current address:
Department of Chemistry, University of Prince Edward Island,
550 University Avenue,
Charlottetown, PEI, C1A 4P3,
Canada.

[c] J. N. Harvey
School of Chemistry, University of Bristol,
Cantock's Close,
Bristol, BS8 1TS
United Kingdom
email: Jeremy.Harvey@bris.ac.uk

## Abstract

It has previously been demonstrated that both [($C_5Me_5$)Ir($PMe_3$)(CH=$CH_2$)H] and [($C_5Me_5$)Ir($PMe_3$)($H_2C$=$CH_2$)] are formed when [($C_5Me_5$)Ir($PMe_3$)] is thermolytically generated in the presence of ethylene. At higher temperatures, the vinyl hydride is converted to the $\eta^2$-ethylene adduct. Density functional theory has now been used to investigate this reaction, using the B3LYP functional, two types of basis sets (LanL2DZ and TZV*) and two models of the [($C_5R_5$)Ir($PR_3$)] species (R = H and $CH_3$). The study consists of full optimizations of local minima, first order saddle points, and minimum energy crossing points (MECP). The experimental results are best accounted for by considering both singlet and triplet spin surfaces. The relative energies of singlet [($C_5R_5$)Ir($PR_3$)($CH_3$)H], [($C_5R_5$)Ir($PR_3$)(CH=$CH_2$)H], and [($C_5R_5$)Ir($PR_3$)($H_2C$=$CH_2$)] are in good agreement with experiment, as is the calculated barrier for the conversion from the vinyl hydride to the $\eta^2$-alkene complex. However, the singlet surface alone fails to explain the experimentally observed product ratio, or the intermediate inferred from experimental isotope effect studies. Locating the MECP between singlet and triplet surfaces indicates that the thermolysis of the singlet alkyl hydride precursor directly forms triplet [($C_5R_5$)Ir($PR_3$)]. The weak van der Waals adduct of triplet [($C_5R_5$)Ir($PR_3$)] and ethylene is proposed to be the key intermediate in the overall reaction. The interchanging of the available ethylene C–H bonds in this triplet σ-complex accounts for the observed kinetic isotope effects, and partitioning between alkene π-complexation and C–H bond activation may also occur from this common intermediate. The possible role of steric factors and molecular dynamics are also discussed.

## Keywords:

Ab initio Calculations; C-H activation; Iridium; Reaction Mechanisms; Spin Crossover

# Introduction

The formation of [Cp*Ir($PMe_3$)($C_6H_{11}$)H] by photolysis of [Cp*Ir($PMe_3$)($H_2$)] in cyclohexane demonstrated the first intermolecular oxidative addition of saturated alkane C-H bonds by a homogeneous organometallic complex.[1] In the years that followed this pioneering report, the reactivity of [Cp*Ir($PMe_3$)] and related [Cp*ML] species (M = Co, Rh, Ir; L = $PR_3$, CO) have been extensively studied experimentally using a variety of kinetic, thermodynamic, and labeling techniques.[2] Simplified [CpML] model complexes have also been subjected to several theoretical analyses, permitting the comparison of different computational techniques. Early work using Extended Hückel molecular orbital (EHMO) theory[3] was followed by studies using density functional theory (DFT), MP2 and other techniques.[4] While the [CpRh(CO)] system has been the most extensively studied,[5] [CpIr($PH_3$)] models for the original Bergman system have also been examined,[5a,6] with the most recent contributions focusing on the later [CpIr($PH_3$)($CH_3$)]$^+$ cationic variants.[7]

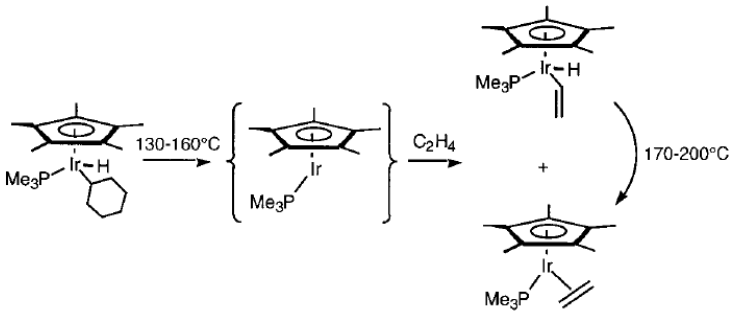


Scheme 1. Thermolysis of [Cp*Ir($PMe_3$)($C_6H_{11}$)H] in cyclohexane.

The reaction shown in Scheme 1 provided the impetus for the current theoretical work. Thermolysis of [Cp*Ir($PMe_3$)($C_6H_{11}$)H] in cyclohexane generates [Cp*Ir($PMe_3$)], which reacts in situ with $H_2C{=}CH_2$ to form [Cp*Ir($PMe_3$)($CH{=}CH_2$)H] and [Cp*Ir($PMe_3$)($H_2C{=}CH_2$)] in a 2:1 ratio.[8] While [Cp*Ir($PMe_3$)($CH{=}CH_2$)H] is stable under the thermolytic conditions of its formation, at higher temperatures it is converted cleanly to [Cp*Ir($PMe_3$)($H_2C{=}CH_2$)]. This remarkable reaction indicates that in contrast to many similar reactions, the ethylene adduct is the thermodynamic product, and can *not* be an intermediate to the vinyl hydride species.

Many reactions of transition metal compounds involve multiple electronic states. We have an ongoing interest in exploring how the associated spin state changes affect the reactivity of organometallic complexes[9] (This has sometimes been referred to as *Two-State Reactivity*[10]). It has long been recognized that the active [CpML] intermediates in CH bond activation processes could possess ground or low-lying excited triplet spin states.[11] Due to the difficulties associated with the theoretical treatment of spin crossover problems, however, the kinetic ramifications of this phenomenon have not been addressed in previous studies. We recently demonstrated the utility of minimum energy crossing point (MECP) locating techniques in evaluating the role of spin state change in organometallic reactions.[12] The system shown in Scheme 1 is of particular interest because the archetypal [Cp*Ir(PMe$_3$)]-based system is of long-standing and ongoing significance for the study of C–H bond activation, and a wealth of experimental and theoretical results are available for these species.[2,4] Furthermore, [CpIr(PH$_3$)] was recently calculated to possess a triplet ground state at various levels of theory.[6] We hereby present extensive B3LYP computations using polarized basis sets on the model [CpIr(PH$_3$)] + C$_2$H$_4$, which, together with additional B3LYP calculations on the full [Cp*Ir(PMe$_3$)(C$_2$H$_4$)] system, provide an explanation for the surprising experimental observations that have resisted rationalization for well over a decade. Our results illustrate the problems involved in using model compounds in computational studies; more importantly, they also demonstrate the importance of singlet-triplet crossover and the powerful way in which locating MECPs can predict its importance.

## Computational Details

Most of the calculations on the [CpIr(PH$_3$)] model, as well as all those relating to the [Cp*Ir(PMe$_3$)] system, were performed using the pseudospectral Jaguar 4.0 package,[13] with a flexible polarized basis set on all atoms. Thus, the Iridium is treated using the Los Alamos relativistic ECP,[14] together with the associated LACV3P++ basis developed for use with Jaguar.[13] The latter basis is a valence triple-zeta contraction of the original double-zeta Los Alamos basis set,[14] augmented by one set of diffuse *d* functions. All other atoms are described by the standard 6-31G basis,[15] with polarization functions (6-31G** basis) on all atoms which can bond to Ir (i.e., the ring C atoms of Cp and Cp*, the P atom, and the whole of the CH$_4$ or C$_2$H$_4$ group). These

calculations will be simply referred to as B3LYP/TZV*. Most of the [CpIr($PH_3$)·($CH_4$)] and [CpIr($PH_3$)($C_2H_4$)] species were also investigated at the B3LYP level using the smaller standard LanL2DZ basis set together with the Gaussian94 program package.[16] The results of these preliminary calculations, where significant, will be briefly mentioned below and referred to as B3LYP/LanL2DZ. The geometries of the minima and transition states were fully optimized without symmetry restrictions, so that convergence to saddle-points during searches for minima, or to higher-order saddle-points during transition state searches should not occur. For transition states, the nature of the transition state was verified by inspecting the unique eigenvector of the approximate Hessian generated during optimization. In a few cases, the exact Hessian was computed, and the expected number of imaginary frequencies was found in all cases. The geometries of the crossing points were also fully optimized, using the method developed by one of the authors,[17] adapted for use with Gaussian or Jaguar. For open-shell species, the Gaussian and Jaguar calculations used unrestricted and restricted open-shell methods, respectively. In all cases, energies are given in kcal $mol^{-1}$ relative to triplet [CpIr($PH_3$)] or [Cp*Ir($PMe_3$)] and $CH_4$ or $C_2H_4$, and do not include a correction for zero-point energy (where available, this correction is found to be small, ~ 1 kcal $mol^{-1}$).

## Results

Our analysis of this reaction relied on a thorough study of the singlet and triplet potential energy surfaces, and of their crossings, using the B3LYP hybrid density functional, together with flexible polarized basis sets. The B3LYP method has proven to be very reliable for a broad range of organometallic systems similar to that studied here.[4] To describe our results, we adopt the following order. First, we briefly summarize the essential experimental observations which we aim to explain, so as to make clear what are the difficulties facing our analysis. We then discuss the electronic structure of the [($C_5R_5$)Ir($PR_3$)] (R = H, Me) intermediate, folllowed by a discussion of the singlet reactive potential energy surface, which, as we will show, is unable to explain the experimental results. Next, we will describe the features of the triplet surface, and finally, we will discuss a realistic scenario for reaction on *both* surfaces, informed by our results concerning the regions where these surfaces cross. Because our main focus is on the reaction of ethylene with the

intermediate, and not the pyrolysis of the cyclohexyl hydride, we have modeled the latter as the smaller methyl hydride.

**Background.**

Thermolysis of [Cp*Ir($PMe_3$)($C_6H_{11}$)H] in the presence of ethylene affords the C-H oxidative addition product [Cp*Ir($PMe_3$)($CH=CH_2$)H] and the ethylene coordinative addition product [Cp*Ir($PMe_3$)($C_2H_4$)] in a 66:34 ratio which is independent of temperature between 130 and 160°C, and is furthermore invariant during the reaction. This observation[8] suggests that the products are obtained via two different transition states and that $\Delta\Delta H^{\ddagger}$ is near zero. Both compounds are thermally stable under the reaction conditions, but thermolysis of the pure vinyl hydride in cyclohexane or benzene at temperatures above 180° results in quantitative conversion to the ethylene complex [Cp*Ir($PMe_3$)($C_2H_4$)]. This confirms that the initially obtained product mixture arising from the activation of ethylene is under kinetic control, and that the ethylene complex cannot be an intermediate along the formation of the C-H oxidative addition product. Also, no phenyl hydride product is observed when the vinyl hydride is converted to the ethylene complex in benzene solvent. This proves that the rearrangement does not involve formation of *free* $C_2H_4$ and [Cp*Ir($PMe_3$)], because independent experiments show that the latter is able to competitively activate benzene and ethylene, and because the benzene activation product, [Cp*Ir($PMe_3$)($C_6H_5$)H], is thermally stable at 180°.

A more detailed kinetic study[18] of the reaction led to some important conclusions. Thus, an activation barrier $\Delta H^{\ddagger}$ of 34.6±1.2 kcal mol$^{-1}$ was found for the rearrangement of [Cp*Ir($PMe_3$)-($CH=CH_2$)H] between 180 and 220°C (with $\Delta S^{\ddagger}$ = 2.6±2.6 eu). The reaction rate was found to be unaffected by the presence of free $PMe_3$, ruling out the involvement of phosphine dissociation. From independent calorimetric studies, a barrier of at least 41 kcal mol$^{-1}$ was estimated for the ethylene reductive elimination from the vinyl hydride, thus confirming that the isomerization process takes place without ethylene reductive elimination.

Intermolecular isotope effects were determined by allowing [Cp*Ir($PMe_3$)] (generated at 145°) to compete for $C_2H_4$ and $C_2D_4$, yielding $k_H/k_D$ = 1.49±0.08 for the formation of the vinyl hydride product and $\delta$ = 0.95±0.02 for the formation of the $\pi$ complex, $\delta$ being the secondary isotope effect that each deuterium has on the rate (for instance $k_H/k_D = \delta^4$ = 0.82±0.05 for the competition between $C_2H_4$ and $C_2D_4$). The intramolecular isotope effects for insertion into C-H and

C-D bonds of the three ethylene-$d_2$ isomers (1,1-, *cis*-1,2-, and *trans*-1,2) were also measured; the values $k_H/k_D$ obtained were identical within experimental error, at 1.18±0.03. These values are not equilibrium isotope effects, because the independently synthesized complex [Cp*Ir($PMe_3$)($CH{=}CH_2$)D] was not found to scramble the label under the same conditions.

The relatively small values of $k_H/k_D$ for the oxidative addition process are consistent with previous reports and with the involvement of an early transition state, where little C-H bond breakage has occurred. The $k_H/k_D$ value for the addition process, when compared with available *equilibrium* isotope effects, indicates that the ethylene structure is perturbed only slightly in the transition state from that found in the free ligand. What is most interesting, however, is that the inter- and intramolecular $k_H/k_D$ for oxidative addition are *not equivalent*. Under the assumption that this difference is not caused by a secondary isotope effect of the non-reacting C-D bonds, *this non-equivalence requires an intermediate on the reaction pathway from which partitioning can occur*. These observations led the authors to propose[18] the existence of an intermediate having the stoichiometry [Cp*Ir($PMe_3$)·($C_2H_4$)] which (a) is not the π-complex [Cp*Ir($PMe_3$)($C_2H_4$)]; (b) is formed upon the intermolecular addition process between [Cp*Ir($PMe_3$)] and $C_2H_4$; and (c) can go on to insert the metal center into any of the four C-H bonds via a unimolecular, intramolecular process. The two mechanistic possibilities A and B illustrated in Scheme 2 were considered. The difference is that the intermediate [Cp*Ir($PMe_3$)·($C_2H_4$)] leads to both the oxidative addition and the π-addition products for mechanism A, while this only affords the oxidative addition product for mechanism B while the π complex is obtained directly by an independent pathway. The product distribution allowed the calculation of the $k_H/k_D$ for each individual step (see Scheme 2). In the event of reversibility for the formation of the [Ir]·($C_2H_4$) intermediate, $k_H/k_D$ for step $k_1$ would be a thermodynamic rather than a kinetic effect. While a rigorous distinction between mechanisms A and B is not possible on the basis of the experimental data, the authors preferred mechanism A because the intermediate presumably involves only weak interactions between the metal center and the C-H bond(s) and a large isotope effect is thus not expected. In addition, the authors were not comfortable with a mechanism in which π-complex formation and C-H oxidative addition require two different transition states.

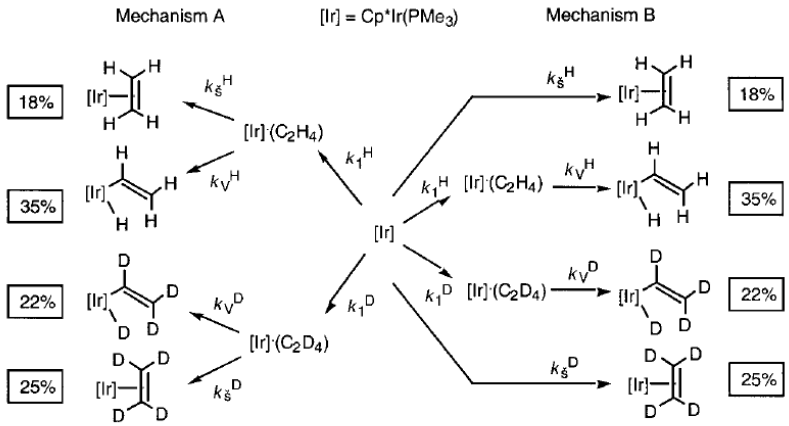


| Step | $k_H/k_D$(Mech.A) | $k_H/k_D$(Mech.B) |
|---|---|---|
| $k_1$ | 1.16 | 1.49 |
| $k_V$ | 1.18 | 1.18 |
| $k_{\ddot{s}}$ | 0.64 | 0.80 |

Scheme 2. The two mechanistic possibilities A and B which account for the existence of an intermediate having the stoichiometry [Cp*Ir($PMe_3$)($C_2H_4$)].

The intermediate required by the energetic (activation) data and isotope studies was proposed to be a metastable species formed by weak coordination of one or more ethylene C-H bonds to the iridium center (σ-complex), with possible structures as shown in Figure 1. The identical intramolecular isotope effects for the different $C_2H_2D_2$ isotopomers, which are different from the intermolecular effect, indicate that the intermediate must be able to chose between all four C-H bonds and forced the authors to propose that several isomeric σ-complexes equilibrate with one another on a time scale which is rapid with respect to conversion to the final products. The authors, however, remained perplexed[18] that this isomerization process seems so facile compared with C-H insertion and π-complex formation.

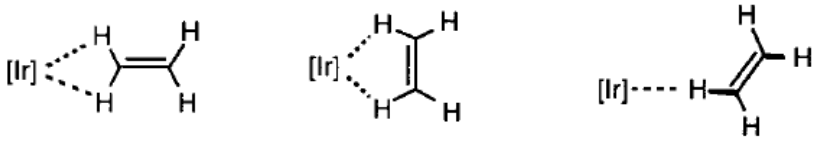


**Figure 1**. Proposed structures[18] for the intermediate on the pathway leading to C-H oxidative addition.

In parallel with the experimental work, some molecular orbital calculations[19] on the model [CpIr($PH_3$)] + $C_2H_4$ system were performed, and led to important insights, but also increased the mystery surrounding it. Whilst the vinyl hydride complex [CpIr($PH_3$)($CH=CH_2$)H] was found to lie

slightly higher in energy than the olefin complex [CpIr($PH_3$)($C_2H_4$)], in agreement with experiment, the initial ethylene coordination step leading to the latter was found to be essentially barrierless, in disagreement with the kinetic preference for the vinyl hydride product. Steric effects and the intervention of multiple spin states were suggested as possible explanations of the results, but could not be explored with the then available computational power.

**Electronic Structure of [CpIr($PH_3$)] and [Cp*Ir($PMe_3$)].**

The assumed intermediate in the reaction studied here is the [Cp*Ir($PMe_3$)] complex, whose electronic structure and geometry are thus of central importance. The qualitative electronic structure of this type of species, based on *ab initio* and density-functional calculations on [CpIr($PH_3$)], has been discussed before in great detail.[6] However, one important feature which has not been fully resolved concerns the relative stability of the singlet and triplet states of this intermediate. A number of theoretical studies, summarized in Table 1, have examined the 16-electron [($C_5H_5$)Ir($PH_3$)] model system, which is relevant to many C-H oxidative addition processes. Because the first *ab initio* study by Ziegler *et al.* predicted a singlet ground state, all subsequent calculations along the methane oxidative addition profile were only carried out on the singlet surface.[5a] This is despite the fact that all subsequent calculations indicate a more stable triplet state.[6] However, no calculations of triplet alkane adducts or transition states or crossing points along the oxidative addition path have been carried out starting from the 16-electron iridium fragment in the triplet state, to the best of our knowledge.

**Table 1.** Computed relative energies of singlet and triplet [($C_5H_5$)Ir($PH_3$)] from this work and previous literature reports.

| $\Delta E_{S-T}$[a)] | Method | ref. |
|---|---|---|
| N.R.(<0)[b)] | Xα | [5a] |
| 33 | ROHF | [6a] |
| 24 | MP2(UHF) | [6a] |
| 26 | CI | [6a] |

| | | |
|---|---|---|
| 20.1 | MP2 | [6b] |
| 20.3 | MP4SDTQ/LanL2DZ// MP2/LanL1DZ | [6b,c] |
| 16.9 | B3LYP/LanL2DZ | [6a] |
| 6.4 | B3LYP/LanL2DZ | this work |
| 8.4 | B3LYP/TZV* | |

[a] E(singlet)-E(triplet) in kcal mol$^{-1}$. [b] Not reported. The singlet is stated to be of lower energy than the singlet (1-6 kcal mol$^{-1}$).

**Table 2.** Energies (in kcal mol$^{-1}$) of all calculated species relative to triplet [CpIr(PH$_3$)] or [Cp*Ir(PMe$_3$)] and CH$_4$ or C$_2$H$_4$.

| Species | [Ir] = [(C$_5$H$_5$)Ir(PH$_3$)] | | [Ir] = (C$_5$Me$_5$)Ir(PMe$_3$) |
|---|---|---|---|
| | B3LYP/LanL2DZ | B3LYP/TZV* | B3LYP/TZV* |
| $^1$[Ir]H(CH$_3$) | -28.1 | -32.3 | -31.3 |
| $^1$[Ir]…CH$_4$ TS | 1.6 | [a] | / |
| $^1$[Ir]·CH$_4$ | 1.1 | [a] | / |
| MECP [Ir]·CH$_4$ | 6.7 | 10.7 | / |
| $^1$[Ir] | 6.4 | 8.4 | 6.8 |
| $^3$[Ir] (E$_{rel}$ = 0)[b] | *-306.42541* | *-641.35249* | *-955.84525* |
| $^1$[Ir]H(C$_2$H$_3$) | -37.2 | -41.2 | -42.8 |
| $^1$[Ir](η$^2$-C$_2$H$_4$) | -46.4 | -51.8 | -49.3 |
| $^1$[Ir](H–C$_2$H$_3$) TS | -5.0 | -7.7 | / |
| $^3$[Ir].C$_2$H$_4$ | -1.2 | -1.1 | / |
| Add. TS to $^3$[Ir](η$^1$-C$_2$H$_4$) | / | 0.8 | / |
| $^3$[Ir](η$^1$-C$_2$H$_4$) | -4.6 | -3.1 | -1.5 |
| $^3$[Ir](η$^1$-C$_2$H$_4$) to η$^2$- TS | 0.07 | -0.3 | / |
| $^3$[Ir](η$^2$-C$_2$H$_4$) | -12.7 | -10.8 | -5.1 |
| $^3$[Ir](H–C$_2$H$_3$) TS | / | 22.8 | / |
| $^3$[Ir]H(C$_2$H$_3$) | / | 9.5 | / |
| MECP nr. $^3$[Ir]·C$_2$H$_4$ | 3.3 | 2.3 | / |
| MECP nr. $^3$[Ir](η$^1$-C$_2$H$_4$) | -2.1 | -2.5 | -1.8 |
| MECP nr. $^3$[Ir](η$^2$-C$_2$H$_4$) | -12.4 | -10.4 | / |

[a] The σ-complex is not a minimum at this level.

[b] The total energies (in Hartrees) for this compound are given for reference purposes.

Our results for [(C$_5$R$_5$)Ir(PR$_3$)] (R = H, Me), as well as all the other calculated B3LYP relative energies are collected in Table 2. For the intermediate, our results are in qualitative agreement with

previous calculations (see Table 1); in particular, the optimized geometries are very close to those previously reported by others and no detailed analysis thereof is warranted here. The Cartesian coordinates of these structures, as well as all other optimized structures reported in this contribution, are deposited as Supporting Information. The triplet is found to be the ground state, but the singlet is fairly low-lying, with excitation energies of 6.4 and 8.4 kcal $mol^{-1}$ for [$CpIr(PH_3)$] at the B3LYP/LanL2DZ* and B3LYP/TZV* levels, respectively; and of 6.8 kcal $mol^{-1}$ for [$Cp^*Ir(PMe_3)$] at the B3LYP/TZV* level. This suggests that crossing to the singlet surface should be relatively facile.

**The Singlet Potential Energy Surface.**

The singlet potential energy surface for the Cp / $PH_3$ model system is shown in Figure 2.

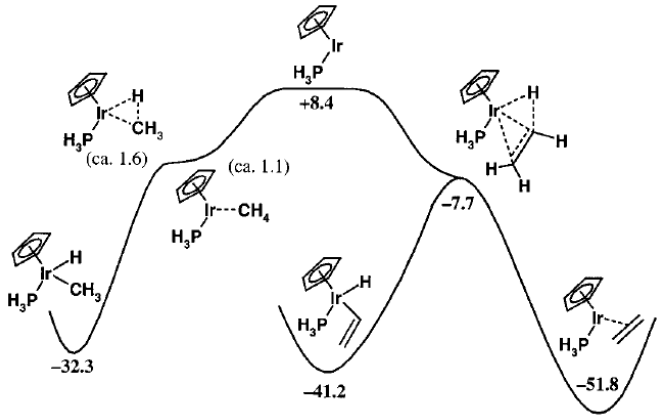


**Figure 2.** Singlet potential energy surface for the process leading from [$CpIr(PH_3)(CH_3)H$] to the ethylene oxidative addition and π-addition products. Energy values (in brackets) are at the B3LYP/TVZ* level in kcal $mol^{-1}$ units.

**Elimination of Methane from Methyl Hydride.** The optimized structures of singlet [$CpIr(PH_3)(CH_3)H$] and [$Cp^*Ir(PMe_3)(CH_3)H$] compare quite closely with previous optimizations and with the experimental structure of [$Cp^*Ir(PMe_3)(C_6H_{11})H$].[20] Our calculations place the [$CpIr(PH_3)(CH_3)H$] model compound 40.7 (34.5) kcal $mol^{-1}$ lower in energy relative to $CH_4$ and singlet [$CpIr(PH_3)$] at the B3LYP/TZV* (B3LYP/LANL2DZ) level (*cf.* 36.3,[5a] 33.5,[6a] 66.0,[6a]

*This value is much smaller than that published in ref. [6c], although they were both derived using the same program, method, and basis set. We have checked our result very thoroughly, and attempted to otherwise explain the discrepancy, without success.

43.1,[6b] and 46.3[6b] obtained at other levels of theory). The real system [Cp*Ir(PMe$_3$)(CH$_3$)H] is calculated as 38.1 kcal mol$^{-1}$ more stable than CH$_4$ and singlet [Cp*Ir(PMe$_3$)] at the B3LYP/TZV* level. We find the barrier for formation of [CpIr(PH$_3$)(CH$_3$)H] from the encounter complex on the singlet surface to be very small, as has also been shown by previous studies.[4] We note that with the single point MP4//MP2 energies of ref. [6b], there is in fact no barrier since the transition state lies lower in energy than the complex. With B3LYP/LanL2DZ, there is a barrier of 0.5 kcal mol$^{-1}$, whereas with B3LYP/TZV*, we do not obtain a distinct [CpIr(PH$_3$)(CH$_4$)] alkane complex: the structure obtained using the smaller basis leads directly to [CpIr(PH$_3$)(CH$_3$)H] upon reoptimization with the larger basis. Within the expected accuracy of our computational method, we cannot predict for sure whether or not there is a barrier of this type, but it would clearly be very small. We note that the intermediacy of a [Cp*Ir(PMe$_3$)·(C$_6$H$_{12}$)] σ-complex has been deduced from kinetic measurements.[21] This does not however prove that there is a barrier on the singlet surface, because the observed complex may be a triplet, with the surface crossing (see below) leading to the observed barrier between it and the alkyl hydride structure. It is also conceivable that there is no barrier to the formation of the encounter complex from the separated 16-electron singlet species and CH$_4$. Thus, the calculated energy for the oxidative addition process would also correspond to the activation barrier for the reductive elimination process to afford the singlet intermediate. No such experimental data has been reported for the elimination of methane, whereas a $\Delta H^{\ddagger}$ value of 35.6 kcal mol$^{-1}$ has been reported for the elimination of cyclohexane from [Cp*Ir(PMe$_3$)(C$_6$H$_{11}$)H].[20]

**Addition of Ethylene to [CpIr(PR$_3$)].** As already discussed by others,[19] there is no barrier to π–addition of ethylene to [CpIr(PH$_3$)] on the singlet surface. To check that this is the case, we performed partial geometry optimizations on the singlet surface whilst fixing the Ir–C distance at successively longer distances. A monotonously increasing potential energy profile is obtained, with the energy computed for fixed r(Ir–C) = 3.56 Å, the longest distance considered, still 5.0 kcal mol$^{-1}$ below the energy of separated [CpIr(PH$_3$)] and ethylene. This effect is larger than could be expected from any computational error and indicates that the interaction between the two moieties is indeed attractive.

Unlike in Hoffmann's computations,[19] however, and as discussed below, there is also no barrier to σ-addition of ethylene to form the vinyl hydride [CpIr(PH$_3$)H(C$_2$H$_3$)]. This is because the

saddle point for interconversion of this species and the ethylene complex lies well below separated [CpIr(PH$_3$)] and ethylene, and is structurally very similar to a σ-complex between the iridium intermediate and ethylene. This finding echoes the result above, whereby methane adds to singlet [CpIr(PH$_3$)] without a barrier.

Based on these findings concerning the singlet potential energy surfaces, it is difficult to explain the experimental observations by Bergman *et al.* The main observation, i.e. the overall 2:1 selectivity for formation of vinyl hydride and ethylene complex, can, it is true, be explained on dynamical grounds as discussed by Hoffmann *et al.*[19] This explanation would loosely run as follows: upon encounter of [CpIr(PR$_3$)] and ethylene, attractive interactions pull the two reagents together. If one of the C–H bonds approaches the iridium center first, and especially if vibrational motion leads to that C–H bond being somewhat more extended than at the equilibrium position, then the system will plunge into the vinyl hydride minimum. If, however, it is mostly the π-bonding orbital of the ethylene which approaches the iridium first, then the ethylene complex will be formed. The preferential formation of vinyl hydride would be accounted for, within this explanation, by subtle features of the "transition region" (meant in the broad sense of the term, since there is no barrier) of the overall attractive [CpIr(PR$_3$)] – ethylene potential energy surface. Molecular dynamics simulations, e.g. using a Car-Parrinello generated *ab initio* potential energy surface,[22] could be used to test this model.

However, even if this model were able to reproduce the observed ratio of products, it would fail to explain the experimental isotope effects. As extensively discussed by Bergman *et al.*,[18] the inter- and intramolecular isotope effects for C–H vs. C–D insertion with $C_2H_4$, $C_2D_4$, 1,1- and *cis* and *trans* 1,2-$C_2H_2D_2$ require that an intermediate [CpIr(PR$_3$)···$C_2H_4$] complex is formed during the reaction.

**Conversion of Vinyl Hydride to η$^2$-Alkene.** The optimized structures of [CpIr(PH$_3$)-(CH=CH$_2$)H] and [CpIr(PH$_3$)($C_2H_4$)], and of the corresponding [Cp*-PMe$_3$] analogues, together with the most relevant bond distances, are shown in Figures 3 and 4, respectively. The structures of the vinyl hydride systems compare favourably with the experimentally determined structure of [Cp*Ir(PMe$_3$)(CH=CH$_2$)H], except that the optimized vinyl C=C distance is significantly longer than experimentally found. This discrepancy has also been recently noted by Hall *et al.*[23] and

attributed to a disorder problem in the experimental structure. A similar phenomenon also seems to occur for the recently reported structure of [Cp*Ir(PMe$_3$)(CH=CH$_2$)Cl].[24] To our knowledge, no experimental structure of a [($\eta^5$-C$_5$R$_5$)Ir(PR$_3$)(R$_2$C=CR$_2$)]-type compounds is available.

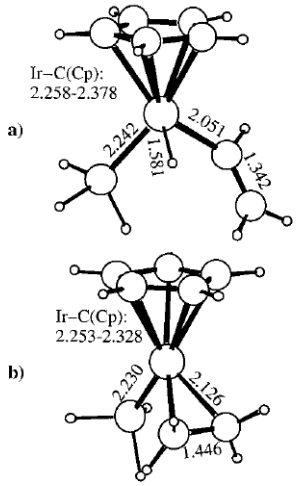


**Figure 3.** B3LYP/TZV* optimized structures of (a) [CpIr(PH$_3$)(CH=CH$_2$)H] and (b) [CpIr(PH$_3$)(C$_2$H$_4$)] with selected bond distances in Å.

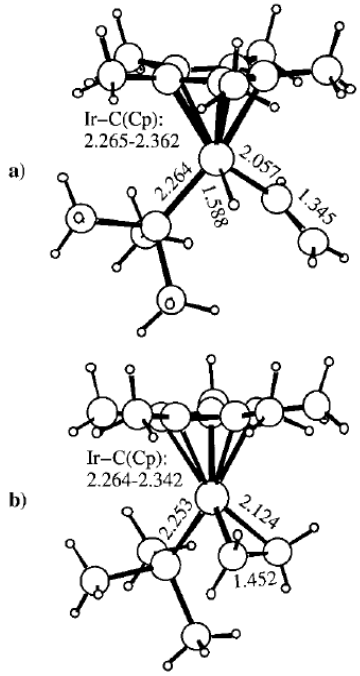


**Figure 4.** B3LYP/TZV* optimized structures of (a) [Cp*Ir(PMe$_3$)(CH=CH$_2$)H] and [Cp*Ir(PMe$_3$)(C$_2$H$_4$)] with selected bond distances in Å.

For both the real and the model system, the ethylene π complex is more stable than the vinyl hydride by several kcal mol$^{-1}$, in agreement with experiment. From calorimetric data, Bergman has estimated a ΔH of 41 kcal mol$^{-1}$ between [Cp*Ir(PMe$_3$)(CH=CH$_2$)H] and [Cp*Ir(PMe$_3$)] + H$_2$C=CH$_2$.[18,24] Our calculations provide 42.8 and 41.2 kcal mol$^{-1}$ for the real and model system,

respectively, relative to the corresponding triplet iridium species. The very similar results on the Cp-$PH_3$ and Cp*-$PMe_3$ systems supports use of simplified models for this aspect of the problem.

The transition state for the isomerization process was only optimized for the model system. The geometry and relevant distances are shown in Figure 5. The distance between Ir and the five individual Cp carbon atoms indicate a significant slipping of the ring toward the $\eta^3$ configuration. This may be because the compound still maintains a certain degree of interaction with the C-H bond while it has already started to establish the interaction with the C-C $\pi$ bonding electrons. This is suggested by the Ir-C-C angle of 106.75° and by the Ir···C distance of 2.956 Å. It is also notable that the geometry of the ethylene moiety is essentially planar and scarcely perturbed with respect to free ethylene. Thus, the transition state can also be viewed as a complex between ethylene and [CpIr($PH_3$)] and it is likely placed on the barrierless reaction pathway leading from singlet [CpIr($PH_3$)] and $C_2H_4$ to either of the compounds separated by the barrier discussed here: [CpIr($PR_3$)H($C_2H_3$)] or [CpIr($PR_3$)($C_2H_4$)] (see Figure 2).

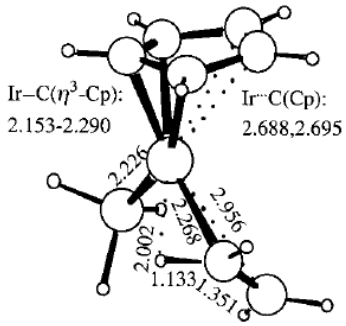


**Figure 5.** B3LYP/TZV* optimized transition state between [CpIr($PH_3$)(CH=$CH_2$)H] and [CpIr($PH_3$)($C_2H_4$)] with selected bond distances in Å.

The calculated energy for this transition state is 7.7 kcal $mol^{-1}$ *below* triplet [CpIr($PH_3$)] + $C_2H_4$ (16.1 kcal $mol^{-1}$ below the corresponding singlet), in agreement with the experimental finding that the rearrangement does not involve ethylene dissociation. This transition state is 33.5 kcal $mol^{-1}$ higher than the vinyl hydride species, in remarkable agreement with $\Delta H^{\ddagger}$ of 34.6 ± 1.2 kcal $mol^{-1}$ for the conversion of [Cp*Ir($PMe_3$)(CH=$CH_2$)H] to [Cp*Ir($PMe_3$)($H_2C$=$CH_2$)].[18]

**The Triplet Potential Energy Surface**

The triplet potential energy surface for the Cp-$PH_3$ model system is shown in Figure 6.

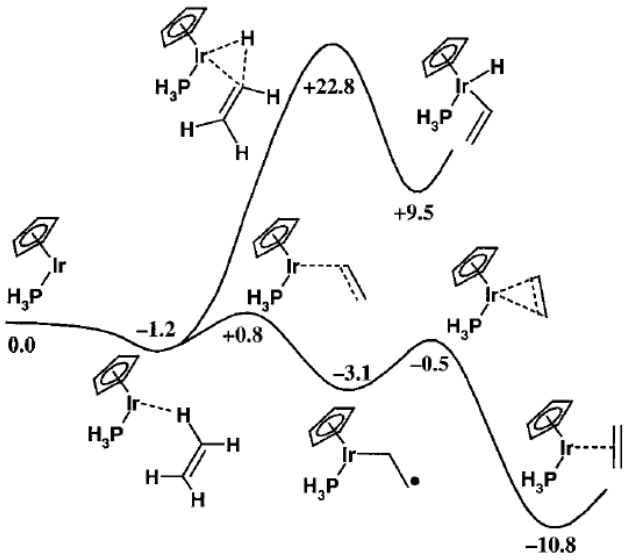


**Figure 6.** Triplet potential energy surface for the interaction between [CpIr($PH_3$)] and ethylene. Energy values are at the B3LYP/TVZ* level in kcal $mol^{-1}$ units.

**Triplet Alkene Complexes.** As noted before, [CpIr($PH_3$)] and [Cp*Ir($PMe_3$)] have triplet ground states, and given the strong spin-orbit coupling in iridium compounds, pyrolysis of alkyl hydrides, even though these species are singlets, will definitely lead to the intermediates in their triplet state. Therefore, in discussing the reactivity with ethylene, the triplet potential energy surface is more relevant when discussing the [CpIr($PR_3$)] intermediate and its encounter complexes than the singlet one.

[CpIr($PH_3$)] forms a weak van der Waals-type complex with ethylene (see Figure 7) which can best be described as a σ-complex. The closest contact between Ir and an ethylene H atom is over 3 Å and the geometry of the [CpIr($PH_3$)] moiety is essentially unperturbed relative to the free fragment. The ethylene molecule approaches the metal from the crowded side of the coordination sphere. The closest distance of the ethylene H atom is in fact to a phosphine H atom (3.245 Å). The weak binding energy (1.1 kcal $mol^{-1}$) of this complex means that the contribution of basis set superposition error (BSSE) to its geometry and binding energy is likely to be substantial. Nevertheless, irrespective of their precise geometry and interaction energy, van der Waals complexes of this type between [Cp*Ir($PMe_3$)] and ethylene will certainly be formed, and, given their very low binding energies, will be able to dissociate and isomerize very readily.

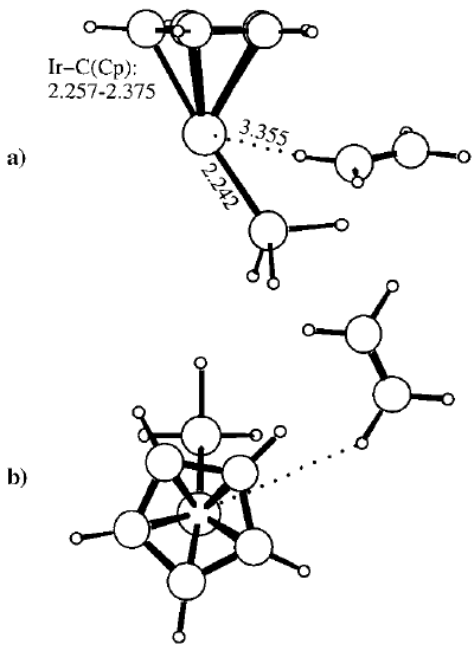


**Figure 7.** Two views of the B3LYP/TZV* optimized structure of the van der Waals complex obtained by the addition of $C_2H_4$ to triplet [$CpIr(PH_3)$].

Triplet [$CpIr(PH_3)$] also forms two covalently bound adducts with ethylene, in which the latter is either $\eta^1$- or $\eta^2$-coordinated. Formation of these adducts involves surmounting small activation barriers. The $\eta^1$ adduct is formed first, *via* what is essentially a radical addition process. Indeed, the $\eta^1$-ethylene complex of triplet [$CpIr(PH_3)$] or [$Cp^*Ir(PMe_3)$] is in a certain sense a radical adduct of the triplet 16-electron complex to ethylene, with one remaining unpaired electron on iridium, a roughly $sp^3$ carbon atom, and an $sp^2$ carbon radical, see Figure 8. The adduct lies at -1.5 and -3.1 kcal $mol^{-1}$ for the real and model systems, respectively, and is separated from reagents by a barrier lying at +0.8 kcal $mol^{-1}$ for the model compound. The ring is essentially symmetric ($\eta^5$) in these species, and the configuration is planar at the metal. That is, the metal sits approximately in the plane defined by the P atom, the ethylene C atom which is bonded to it, and the center of gravity of the cyclopentadienyl ligand. As can be appreciated from Figure 8, the "radical-type" C atom has a planar configuration. It is interesting to note the different orientation of the $\eta^1$-$C_2H_4$ ligand, which appears to prefer a "vertical" position in the less hindered model compound, whereas it is more "horizontal" in the real system. Although the barrier to rotation between the Ir and the $sp^3$-hybridized C atom is obviously rather small, the much greater steric bulk of the ligands in the real system does appear to somewhat destabilize this adduct, which is 3.1 kcal $mol^{-1}$ below reagents for the model, but only 1.5 kcal $mol^{-1}$ below for the real system.

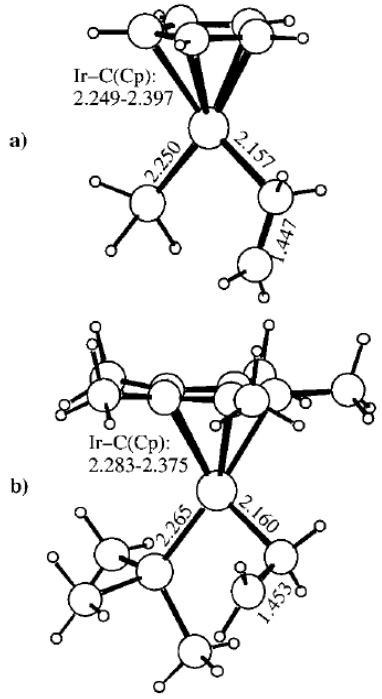


**Figure 8.** B3LYP/TZV* optimized structures of (a) [CpIr($PH_3$)($\eta^1$-$C_2H_4$)] and (b) [Cp*Ir($PMe_3$)($\eta^1$-$C_2H_4$)] in the triplet state, with selected bond distances in Å.

In a second step, this species forms a second Ir-C bond to afford an $\eta^2$ ethylene complex, see Figure 9, with this being the lowest energy species on the triplet surface. As in the model system $\eta^1$ adduct, but unlike the singlet ethylene complex, the ethylene is bound in a "vertical" configuration, with the C–C bond orthogonal to the $C_5R_5$ plane. Also, the cyclopentadienyl undergoes ring-slipping and is only $\eta^3$-coordinated to iridium, presumably because an $\eta^5$ configuration leads to an 18 electron species, which is not possible for a triplet. This conformational change may contribute to the small computed barrier for the rearrangement process, which lies 0.3 kcal $mol^{-1}$ *below* the separated triplet [CpIr($PH_3$)] and ethylene. The configuration at the metal is again planar, like for the $\eta^1$-ethylene triplet species.

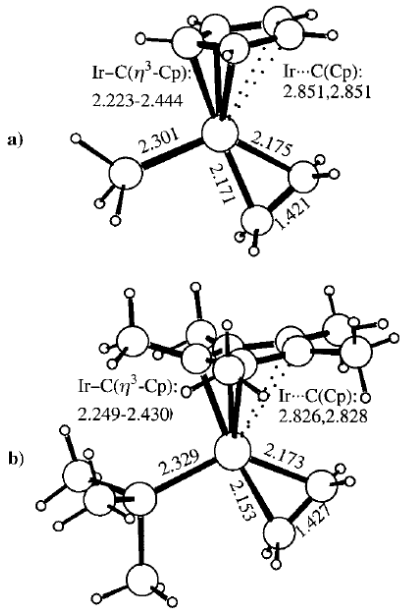


**Figure 9.** B3LYP/TZV* optimized structures of (a) [CpIr($PH_3$)($\eta^2$-$C_2H_4$)] and (b) [Cp*Ir($PMe_3$)($\eta^2$-$C_2H_4$)] in the triplet state, with selected bond distances in Å.

Unlike the $\eta^1$ adduct, the ethylene ligand in this $\eta^2$ complex is "vertical" in the real system as well as in the model, indicating that the electronic preference for this orientation is much stronger in this case. As a result, the relative energy of this intermediate is quite strongly affected by the increased steric bulk of the [Cp*Ir($PMe_3$)] system. Thus, [Cp*Ir($PMe_3$)($\eta^2$-$C_2H_4$)] lies only 5.1 kcal $mol^{-1}$ below [Cp*Ir($PMe_3$)], compared to 10.8 in the [CpIr($PH_3$)] model system. The reason for this substantial destabilization can be readily understood upon considering the optimized structure. Thus, the "vertically" coordinated ethylene ligand is very close to the methyl groups of the $PMe_3$ and Cp* groups, with the shortest H–H contacts being of respectively 2.54 and 2.46 Å. In this case, the use of the model compound is therefore somewhat misleading. With the increasing computing power available nowadays, many such cases are being observed where the use of model compounds leads to incorrect conclusions as here.[25, 26]

Overall, there seems to be an increasing amount of steric yield as one goes from the van der Waals triplet complex to the $\eta^1$ then $\eta^2$-complexes. Although we have not located the two corresponding transition states for the real system, steric hindrance will probably act on them too, so that they will lie somewhat higher in energy than in the model [CpIr($PH_3$)] system. This means that the $\eta^1$ and especially $\eta^2$ adducts may be formed less readily than may be assumed upon looking at the potential energy surface of Figure 6: crossover to the singlet surface (see below) can occur from

both the van der Waals and $\eta^1$ adducts, and this process will compete with barrier crossing on the triplet surface.

**Triplet Insertion Chemistry.** Given that [Cp*Ir($PMe_3$)] is expected to be formed in its triplet state, one should also consider the possibility that C–H insertion to form the vinyl hydride product can occur upon the triplet potential energy surface. This is indeed possible, but as shown in Fig. 6, the triplet vinyl hydride is less stable than the reagents, lying at +9.5 kcal mol–1, and the corresponding transition state is extremely high, at 22.8 kcal $mol^{-1}$. Clearly, this route is not compatible with the experimental observations.

Overall, the experimental observations of Bergman *et al.* cannot be explained by considering the triplet surface alone, just as they could not be reconciled with the features of the singlet surface. Instead, one must consider both surfaces *together*, and the regions of configurational space where the two lie close in energy, as discussed below.

**Singlet-Triplet Surface Crossings - MECPs**

For compounds containing transition metals, especially those from the third row such as iridium, potential energy surfaces corresponding to wavefunctions of defined electronic spin are often not a good description of the system, and are often not particularly useful even as zero-order representations. This is because the corresponding wavefunctions are *diabatic* states, i.e. they are not eigenfunctions of the full Hamiltonian of the system, which includes spin-orbit coupling, and has *adiabatic* eigenstates for which the electronic spin is not well defined. In the present system, the high spin-orbit coupling due to the iridium atom will lead to substantial mixing between the singlet and triplet states for many of the geometries discussed here. Therefore, the reactions in this system may well occur in a completely *adiabatic* manner, passing smoothly from regions where the wavefunction is mostly singlet in nature to regions where it is mostly triplet, and then back to singlet in the product region. Although this requires passing from the singlet diabatic surface to the triplet surface, this spin-forbidden character may not impede the reaction in any significant way.[†] The most appropriate *ab initio* method for the study of the mechanism of such processes would be

[†]Obviously, the situation may be different for systems containing only second- or expecially first-row transition metal atoms, as discussed elsewhere (ref. [9c]).

one which included spin-orbit coupling in the corresponding Hamiltonian, instead of just treating the kinetic energy and Coulomb terms.

However, such methods are not available, especially when one takes into account additional difficulties such as the large number of atoms in the system, scalar relativistic effects, correlation, etc. Therefore, one must make do with computational studies of the individual spin states. For systems such as the present one, where the crossing from one surface to another occurs in a mechanistically important region of the global potential energy surface, it is not enough to locate stationary points (minima, transition states) on each surface separately, as is usually done. One must also find the relevant minimum energy crossing points (MECPs) between surfaces, which represent the energy barriers the system needs to cross in the zero-order representation of the potential energy surfaces. Of course, strong spin-orbit coupling will mix the surfaces to a considerable extent around the MECPs, but even so, their geometries and relative energies provide insight, at least at the semi-quantitative level, into the features of the adiabatic spin-coupled potential energy surface.

We discuss below four regions where the singlet and triplet surfaces cross, and how this may affect reactivity. Most of these MECP calculations have only been carried out on the less expensive Cp-$PH_3$ model system. However, one of the MECPs was studied for the real system, and this led to a very similar result to that obtained with the model. We note that the present procedure to characterize surface crossings, explicit optimization of the MECP without geometry restrictions, was shown in ref. XX to be faster and more accurate than previously used "partial optimization" techniques leading to rough lower and upper boundaries on the energy of the MECP.

**MECP at [CpIr($PH_3$)($CH_4$)] or [CpIr($PH_3$)].** The first significant crossing of the singlet and triplet surfaces occurs in the vicinity of the [CpIr($PH_3$)] complex with methane. We find a crossing lying just above the singlet dissociation asymptote. The geometry of this crossing, shown in Figure 10, has the $CH_4$ moiety far from the transition metal center, so that it does not really play a significant role in mediating the crossing of the two surfaces. In fact, the [CpIr($PH_3$)] system itself at the geometry of this MECP, but with the methane atoms omitted, is very close to an MECP as judged from the energy splitting and effective gradient. The Cp adopts a $\eta^5$ coordination mode but is slightly asymmetric, the three C atoms directly opposite to the $PH_3$ being significantly farther as a

probable result of trans influence. The configuration at the metal is off planar, as can better be appreciated from the perpendicular view on Figure 10(b).

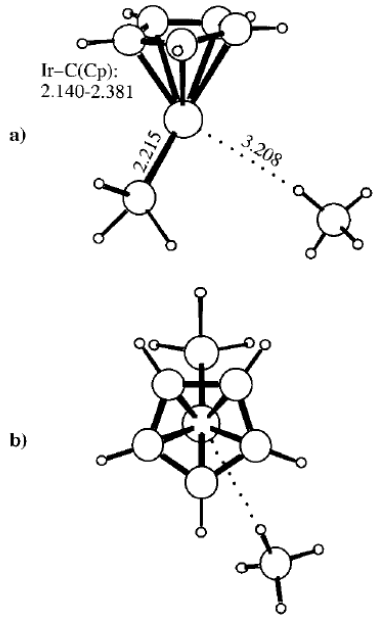


**Figure 10.** Two different views of the B3LYP/TZV* optimized MECP leading to triplet [CpIr($PH_3$)] by $CH_4$ reductive elimination from [CpIr($PH_3$)($CH_3$)H].

The energy of the crossing found here is slightly above that of singlet [CpIr($PH_3$)]. This means that surface crossing will not substantially accelerate alkane dissociation with respect to the spin-allowed reaction, unlike the situation found in other cases.[12] However, if one takes into account the strong iridium spin-orbit coupling, and the low energy of the MECP relative to the singlet minimum, it is clear that [CpIr($PH_3$)] will have a very short lifetime (or none at all if crossing occurs during the late stages of the dissociation) before relaxing to the triplet state. Thus, the singlet intermediate will not have time to react with other species, e.g. ethylene. In practical terms, pyrolysis of the methyl or cyclohexyl hydride will directly lead to [CpIr($PH_3$)] (or [Cp*Ir($PMe_3$)]) in its triplet ground state.

The next three MECPs are in the vicinity of the three [CpIr($PH_3$)] + ethylene triplet minima discussed above. Indeed, unlike methane, which does not significantly alter the position of the MECP between singlet and triplet [CpIr($PH_3$)], ethylene leads to qualitatively new MECPs in which the ethylene moiety is very close to the iridium atom.

**MECP near [CpIr(PH3)] + ethylene van der Waals adduct.** This structure is shown in Figure 11, and lies at +2.3 kcal mol$^{-1}$. It can be seen to be rather similar in geometry to the transition state converting the singlet vinyl hydride and the ethylene adduct (Figure 5). In fact, geometry optimization on the singlet potential energy surface starting at this MECP leads to the vinyl hydride compound, suggesting that if crossover occurs in this region of configurational space, formation of the vinyl hydride product will be favored. Unlike the TS in Figure 5, however, the MECP in Figure 11 shows a more symmetric $\eta^5$ coordination mode for the Cp ligand. In addition, the second ethylene carbon is further away from the Ir atom (3.143 Å) and the Ir-C-C angle is much more open (119.50°) relative to the TS in Figure 5. Equally, the ethylene structure at this MECP is scarcely changed with respect to its optimal geometry, so there should be no additional barrier separating this MECP from separated [CpIr(PH3)] and ethylene.

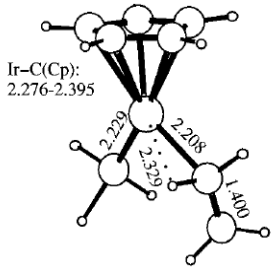


**Figure 11.** B3LYP/TZV* optimized MECP in the triplet [CpIr(PH3)·(C2H4)] region, leading to singlet [CpIr(PH3)(CH=CH2)H].

**MECP near [CpIr(PH3)(η1-H2C=CH2)].** This MECP, shown in Figure 12, lies at -2.5 kcal mol$^{-1}$ and is similar in geometry to the $\eta^1$ triplet adduct (Figure 7).‡ No clear indication of an Ir···H interaction is shown in this structure, since the Ir is symmetrically disposed over the sp$^3$ hybridized C atom (Ir-C-C = 109.87°). On the other hand, the Ir···C separation to the second ethylene C atom is shorter than in the triplet $\eta^1$-C2H4 adduct of Figure 7 (2.972 vs. 3.088 Å), indicating an incipient

‡ The triplet $\eta^1$ adduct of ethylene with [Ir] has one unpaired electron on iridium, and one on the distal carbon atom of the ethylene group. Spin-coupling between these two electrons should be fairly weak, so that there should be an open-shell singlet state very close in energy. Using *restricted* B3LYP, the closed-shell singlet lies 15.7 kcal mol$^{-1}$ above the triplet at its minimum. Using *unrestricted* B3LYP, and the method of Noodleman *et al.* [ref. 27], the open-shell singlet can be estimated to lie just 4.0 kcal mol$^{-1}$ higher than the triplet. For most other species discussed here, however, the lowest energy singlet should be closed-shell in nature. For example, UB3LYP computations predict open-shell $^1$[Ir] to lie 12.4 kcal mol$^{-1}$ above the triplet - 4.0 kcal mol$^{-1}$ higher than the closed-shell singlet. Nevertheless, the fact that we use RB3LYP to compute singlet states does mean that some regions of the potential energy surface may not be quantitatively accurate. However, this is expected to play a far less important role than spin-orbit coupling, and should have no bearing on our qualitative results.

interaction. Indeed, optimization from this point leads to the π-ethylene adduct, suggesting that that product would be formed if crossover occurs in that region. To reach this MECPs, it is necessary to first cross the low barrier leading to the $\eta^1$ ethylene adduct. The geometry of this MECP was also optimized for the real [Cp*Ir($PMe_3$)] system. The geometry is similar to that found for the model. The relative energy is very slightly higher, in line with the slight destabilization of [Cp*Ir($PMe_3$)($\eta^1$-$C_2H_4$)] compared to [CpIr($PH_3$)($\eta^1$-$C_2H_4$)].

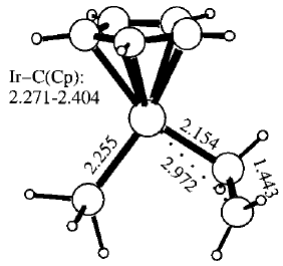


**Figure 12.** B3LYP/TZV* optimized MECP leading from triplet [CpIr($PH_3$)($\eta^1$-$C_2H_4$)] to singlet [CpIr($PH_3$)($\eta^2$-$C_2H_4$)].

**MECP near [CpIr($PH_3$)($\eta^2$-$H_2C$=$CH_2$)].** As discussed separately above, the singlet and triplet $\eta^2$-ethylene complexes have very different structures, with the ethylene lying "horizontally" in the former, and "vertically" in the latter. This might suggest that the triplet complex, which lies well above the singlet in energy, may not be able to relax very efficiently to the singlet. In fact, the singlet state is very close in energy to the triplet at the triplet minimum geometry, and there is an MECP lying close in geometry (shown in Figure 13, *cf.* with Figures 9a) and energy (see Table 2). Likewise, the MECP should be close in energy and geometry to the corresponding triplet minimum for the "real" system. Therefore, if the triplet [Cp*Ir($PMe_3$)($\eta^2$-$H_2C$=$CH_2$)] complex is formed, it should be readily able to cross over to the singlet surface, leading to the global minimum, singlet [Cp*Ir($PMe_3$)($\eta^2$-$H_2C$=$CH_2$)].

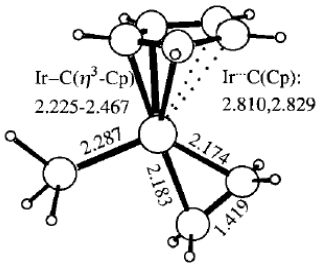

**Figure 13.** B3LYP/TZV* optimized MECP leading from triplet [CpIr($PH_3$)($\eta^2$-$C_2H_4$)] to singlet [CpIr($PH_3$)($\eta^2$-$C_2H_4$)].

**Discussion.** There are many regions of the potential energy surface in the [CpIr($PH_3$)] + ethylene region where the singlet and triplet states are near degenerate, and we have located three MECPs. From two of these, the steepest descent route leads to the singlet ethylene compound, and from the third, one reaches the vinyl hydride compound. Since this third MECP is the highest in energy, and in fact lies somewhat above the energy of the reagents, one could conclude that our calculations predict the sole formation of singlet [CpIr($PH_3$)($\eta^2$-$H_2C$=$CH_2$)], which would disagree with experiment.

In fact, this is not the case for several reasons. First of all, the highest-lying MECP, from which the steepest-descent path leads to the vinyl hydride product, is the only one which can be reached directly from the triplet ethylene van der Waals complex. The other two MECPs are only reached after crossing one or two transition states. Although these transition states are low-lying for the model system studied here, they may lie somewhat higher for the real system. In particular, the MECP which is close to the triplet $\eta^2$-ethylene complex, and which from a first glance would be the easiest way in which to reach the singlet surface, may not be significantly involved in the reaction. This is because the transition state leading to the triplet $\eta^2$-ethylene complex, and this complex itself, are subject to quite severe steric hindrance from the methyl groups on Cp* and $PMe_3$ in the "real" [Cp*Ir($PMe_3$)] system. In this case, therefore, the use of a model compound to derive the reaction profile is slightly misleading, although the effect is less dramatic than has sometimes been observed [ref GGG].

Secondly, although the two other MECPs differ in that the direct downhill route from them leads to different products, they are not entirely dissimilar in geometry, and both are fairly similar to the singlet transition state separating the two products. Also, they both lie *higher* in energy than that transition state. This means that the seam of crossing between the two surfaces must lie at fairly low energies across quite a broad region of the potential energy surface and that the system may be able to cross in many places, not restricted to the immediate vicinity of the two MECPs we have located. It also means that once the system does cross onto the singlet surface, how it partitions between the vinyl hydride and the ethylene complex may be determined to a large extent by the dynamics, rather

than by the nature of the steepest descent path. As discussed above, this dynamical question would require much more work to investigate.

Finally, one has to realize that a product ratio of 2:1 corresponds to a very small difference in free energy between the two pathways, and that the computational difficulties in a system such as the present one are simply too challenging for one to be able to predict the outcome quantitatively.

Given these provisos, the general picture emerging from our calculations (see Figure 14) *is* in agreement with the experimental observations. Thus, our calculations predict the following, based on the features of the singlet and triplet surfaces, and of their intersections:

* Heating [Cp*Ir(PMe$_3$)H(C$_6$H$_{11}$)] will lead to loss of cyclohexane, and formation of [Cp*Ir(PMe$_3$)] in its ground, triplet state. This is due to the fact that a crossing between singlet and triplet surfaces occurs very close in energy to the singlet state.

* The triplet will interact with ethylene to form a weakly bound van der Waals adduct. Given the low interaction energy in this intermediate, it will be able to interconvert readily, in agreement with the isotope effect data. It is worth to mention here that the calculated geometry of this intermediate is as predicted in the experimental study,[18] except for the spin state.

* Addition to form triplet $\eta^1$- and $\eta^2$-ethylene adduct may also occur, although there are barriers for formation of these species, especially the latter one. In the model system, where we have optimized the corresponding transition states, these barriers are very low, but they are predicted to be somewhat higher in the real system.

* The singlet surface intersects the triplet surface at multiple points, all lying at relatively low energy, so that crossover to the singlet state should be relatively facile. However, the surface crossing will lead to small barriers, and thus to a finite lifetime for the triplet intermediates. It is hard to predict the ratio of products on the singlet surface. In particular, because the transition state which separates [Cp*Ir(PMe$_3$)($\eta^2$-C$_2$H$_4$)] and [Cp*Ir(PMe$_3$)(CH=CH$_2$)H] is *lower* in energy than the relevant surface crossings, dynamical factors will affect to which side of this partitioning barrier the system will fall. Thus, although our results are at first sight suggestive of the ethylene complex being preferentially formed, upon close consideration, especially concerning the uncertainties involved, the results are compatible with the observed 2:1 ratio in favor on the vinyl hydride.

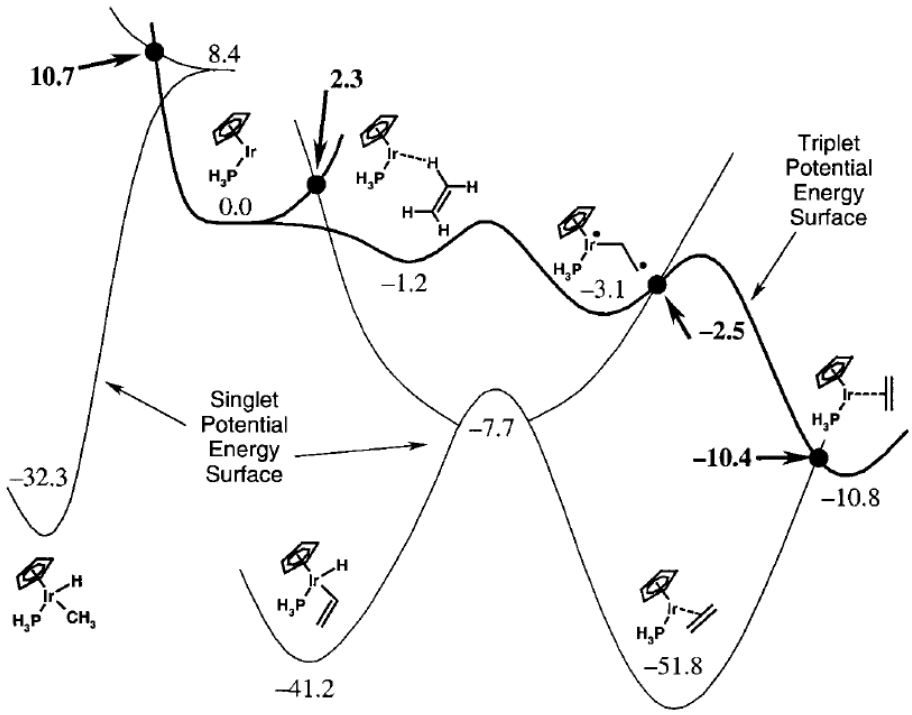


**Figure 14.** Schematic drawing showing the four MECPs between singlet and triplet potential energy surfaces, and thereby the two-state pathway leading from singlet [CpIr($PH_3$)H($CH_3$)] to singlet [CpIr($PH_3$)H(CH=$CH_2$)] or singlet [CpIr($PH_3$)($\eta^2$-CH=$CH_2$)] *via* triplet [CpIr($PH_3$)]. Relative energies in kcal $mol^{-1}$.

**Acknowledgement.** R.P. and JNH thank the Région Bourgogne and the EPSRC (Grant M92089), respectively, for supporting this research; and K.M.S. thanks the European Commission for a TMR Marie Curie Postdoctoral Fellowship.

**Supporting Information** Cartesian coordinates of all calculated complexes.

## References


[1] A. H. Janowicz, R. G. Bergman, *J. Am. Chem. Soc*. **1982**, *104*, 352–354.

[2] a) B. A. Arndsten, R. G. Bergman, T. A. Mobley, T. H. Peterson, *Acc. Chem. Res.* **1995**, *28*, 154–162; b) A. E. Shilov, G. B. Shul'pin, *Chem. Rev.* **1997**, *97*, 2879–2932.

[3] a) P. Hofmann, M. Padmanabhan, *Organometallics* **1983**, *2*, 1273–1284; b) J.-Y. Saillard, R. Hoffmann, *J. Am. Chem. Soc*. **1984**, *106*, 2006–2026.

[4] S. Niu, M. B. Hall, *Chem. Rev.* **2000**, *100*, 353–405.

[5] CpRh(CO): a) T. Ziegler, V. Tschinke, V.-Y. Fan, A. D. Becke, *J. Am. Chem. Soc*. **1989**, *111*, 9177–9185; b) J. Song, M. B. Hall, *Organometallics* **1993**, *12*, 3118–3126, c) D. G. Musaev, K. Morokuma, *J. Am. Chem. Soc*. **1995**, *117*, 799–805; d) P. E. M. Siegbahn, *J. Am. Chem. Soc*. **1996**, *118*, 1487–1496; e) M.-D. Su, S.-Y. Chu, *Organometallics* **1997**, *16*, 1621–1627.

[6] CpIr($PH_3$): a) R. Jiménez-Cataño, M. B. Hall, *Organometallics* **1996**, *15*, 1889–1897; b) M.-D. Su, S.Y. Chu, *J. Phys. Chem. A* **1997**, *101*, 6798–6806; c) M. D. Su, S. Y. Chu, *Chem. Eur. J*. **1999**, *5*, 198–207.

[7] [CpIr($PH_3$)($CH_3$)]$^+$: a) D. L. Strout, S. Zaric, S. Niu, M. B. Hall, *J. Am. Chem. Soc*. **1996**, *118*, 6068–6069. b) M.-D. Su, S.-Y. Chu, *J. Am. Chem. Soc*. **1997**, *119*, 5373–5383. c) C. Hinderling, D. Feichtinger, D. A. Plattner, P. Chen, *J. Am. Chem. Soc*. **1997**, *119*, 10793–10804. d) S. Niu, M. B. Hall, *J. Am. Chem. Soc*. **1998**, *120*, 6169–6170.

[8] P. O. Stoutland, R. G. Bergman, *J. Am. Chem. Soc*. **1985**, *107*, 4581–4582.

[9] a) R. Poli, *Chem. Rev*. **1996**, *96*, 2135–2204; b) R. Poli, *Acc. Chem. Res*. **1997**, 30, 494–501; c) J. N. Harvey, in *Computational Organometallic Chemistry*, T. C. Cundari, ed.: Marcel Dekker, in press.

[10] For other work in this area, see D. Schröder, S. Shaik, H. Schwarz, *Acc. Chem. Res.* **2000**, *33*, 139–145.

[11] A. H. Janowicz, H. E. Bryndza, R. G. Bergman, *J. Am. Chem. Soc*. **1981**, *103*, 1516–1518.

[12] K. M. Smith, R. Poli, J. N. Harvey, *New J. Chem.* **2000**, *24*, 77–80.

[13] Jaguar 4.0, Schrödinger, Inc., Portland, OR, 1991 - 2000.

[14] P. J. Hay, W. R. Wadt, *J. Chem. Phys.* **1985**, *82*, 299 – 310.

[15] P. C. Hariharan, J. A. Pople, *Mol. Phys.* **1974**, *27*, 209 – 214.

[16] M. J. Frisch, G. W. Trucks, H. B. Schlegel, P. M. W. Gill, B. G. Johnson, M. A. Robb, J. R. Cheeseman, T. Keith, G. A. Petersson, J. A. Montgomery, K. Raghavachari, M. A. Al-Laham, V. G. Zakrzewski, J. V. Ortiz, J. B. Foresman, J. Cioslowski, B. B. Stefanov, A. Nanayakkara, M. Challacombe, C. Y. Peng, P. Y. Ayala, W. Chen, M. W. Wong, J. L. Andres, E. S. Replogle, R. Gomperts, R. L. Martin, D. J. Fox, J. S. Binkley, D. J. Defrees, J. Baker, J. P. Stewart, M. Head-Gordon, C. Gonzalez and J. A. Pople, *Gaussian 94 (Revision E.1)*; Gaussian Inc.: Pittsburgh, PA, 1995.

[17] a) J. N. Harvey, M. Aschi, H. Schwarz, W. Koch, *Theor. Chem. Acc.*, **1998**, *99*, 95–99; b) J. N. Harvey, M. Aschi, *Phys. Chem., Chem. Phys.* **1999**, *1*, 5555–5563.

[18] P. O. Stoutland, R. G. Bergman *J. Am. Chem. Soc.* **1988**, *110*, 5732−5744.

[19] J. Silvestre, M. J. Calhorda, R. Hoffmann, P. O. Stoutland, R. G. Bergman, *Organometallics* **1986**, *5*, 1841−1851.

[20] J. M. Buchanan, J. M. Stryker, R. G. Bergman, *J. Am. Chem. Soc.* **1986**, *108*, 1537−1550.

[21] P. O. Stoutland, R. G. Bergman, S. P. Nolan, C. H. Hoff, *Polyhedron* **1988**, *7*, 1429−1440.

[22] For a review of this approach, see T. K. Woo, P. M. Margl, L. Deng, L. Cavallo, T. Ziegler, *Catalysis Today*, **1999**, *50*, 479–500.

[23] M. B. Hall, S. Niu, J. H. Reibenspies, *Polyhedron* **1999**, *18*, 1717−1724.

[24] S. N. Paisner, P. Burger, R. G. Bergman, *Organometallics* **2000**, *19*, 2073−2083.

[25] See e.g. a) H. Jacobsen, H. Berke, *Chem. Eur. J.* **1997**, *3*, 881–886; b) T. Hascall; D. Rabinovich, V. J. Murphy, M. D. Beachy, R. A. Friesner, G. Parkin, *J. Am. Chem. Soc.* **1999**, *121*, 11402–11417.

[26] Steric effects with large, realistic ligands can also be studied computationally using QM/MM methods. For a review, see Maseras, F., *Chem. Commun.* **2000**, *19*, 1821–1827.

[27] L. Noodleman, D. A. Case, A. Aizman, *J. Am. Chem. Soc.* **1988**, *110*, 1001–1005.

**Suggested Table of Contents Entry (Text):**

The unusual pattern of reactivity in addition of ethylene to [Cp*Ir(PMe$_3$)] led Bergman to label it a *mysterious reaction*. Our DFT study of the singlet and triplet hypersurfaces, including the spin crossover points (one of which is shown here), shows that the experimental results can only be rationalized by a Two State Reaction pathway involving triplet intermediates.